Hydrol. Earth Syst. Sci. Discuss., 10, 11901–11941, 2013
www.hydrol-earth-syst-sci-discuss.net/10/11901/2013/
doi:10.5194/hessd-10-11901-2013

Hydrology and Earth System Sciences
Discussions

A conceptual model of check dam hydraulics for gully control

C. Castillo[1,2], **R. Pérez**[2], **and J. A. Gómez**[1]

[1]Institute for Sustainable Agriculture, CSIC, Apartado 4084, 14080 Cordoba, Spain
[2]University of Cordoba, Dept. of Rural Engineering, Campus Rabanales, Leonardo Da Vinci Building, 14071 Cordoba, Spain

Received: 17 July 2013 – Accepted: 4 September 2013 – Published: 30 September 2013

Correspondence to: C. Castillo (ccastillo@ias.csic.es)

Published by Copernicus Publications on behalf of the European Geosciences Union.

Abstract

There is little information in scientific literature regarding the modifications induced by check dam systems in flow regimes in restored gully reaches, despite it being a crucial issue for the design of conservation measures. Here, we develop a conceptual model to classify flow regimes in straight rectangular channels for initial and dam-filling conditions as well as a method of estimating efficiency in order to provide guidelines for optimal design. The model integrates several previous mathematical approaches for assessing the main processes involved (hydraulic jump HJ, impact flow, gradually varied flows). Its performance was compared with the simulations obtained from IBER, a bi-dimensional hydrodynamic model. The impact of check dam spacing (defined by the geometric factor of influence c) on efficiency was explored. Eleven main classifications of flow regimes were identified depending on the element and level of influence. The model produced similar results when compared with IBER, but led to higher estimations of HJ and impact lengths. Total influence guaranteed maximum efficiency and HJ control defining the location of the optimal c. Geometric total influence ($c = 1$) was a valid criterion for the different stages of the structures in a wide range of situations provided that hydraulic roughness conditions remained high within the gully, e.g. through revegetation. Our total influence criterion involved shorter spacing than that habitually recommended in technical manuals for restoration, but was in line with those values found in spontaneous and stable step-pools systems, which might serve as a reference for man-made interventions.

1 Introduction

A check dam is a small dam designed to reduce flow velocity and to enhance sediment deposition in order to control soil erosion within a stream, such as a gully. Although there are examples of successful projects in gully restoration using check dams, e.g. Alcali Creek Project (Weinhold, 2007), on numerous occasions faults have been

reported in the performance of these structures (Heede, 1960; Iroume, 1996; Nyssen et al., 2004), including channel degradation and scouring downstream of the check dams (Porto and Gessler, 2000; Castillo et al., 2007; Conesa-García et al., 2007). Consequently, for a successful gully restoration, it would be necessary to describe the main hydraulic modifications produced by check dams in the water flow in order to design these structures effectively so that their stability is guaranteed in the long-term.

Several approaches have contributed greatly to the understanding of some of the essential processes in drop structures, such as hydraulic jump and waterfall impact (Rand, 1955; Vischer and Hager, 1995; Chanson, 1999), allowing a precise characterization of dissipation phenomena. Physically-based hydraulic models have been used to evaluate flood regimes and the influence of channel geometry in ephemeral channels in arid regions (Merrit and Wohl, 2001) and may become a useful tool for contrasting the performance of conceptual models which aim to predict the free-surface water profiles in gullies controlled by hydraulic structures. In fact, the different criteria proposed for determining the spacing between adjacent check dams derive from observations of water flow in natural and artificial channels, although there is no single universally accepted criterion. The three criteria most commonly found in the literature are: (a) the head-to-toe criterion, namely, the toe of the upstream dam is at the same elevation as the top of the downstream dam (Heede, 1960); (b) the ultimate slope criterion defining an equilibrium slope for incipient sediment motion (Porto and Gessler, 1999); (c) empirical observations of the sediment deposit gradient in restored channels (Heede, 1978; Iroume and Gayoso, 1991). It is apparent that there are great differences in these recommendations, despite the fact that spacing is a critical factor for check dam design, and this leads to an undesirable degree of technical uncertainty.

The analogy between step-pool systems and check dam interventions has been recently recognized, to the point that check dams have been considered as the anthropogenic equivalent to step-pool sequences in steep mountain streams (Milzow, 2004). Step-pool morphological features have inspired the design criteria for artificial check dam sequences in high-gradient streams stabilization (Lenzi, 2002; Wang and

Yu, 2007; Chin et al., 2009). Step-pools represent an interesting case of spontaneous, self-organized system of high stability (Chin and Phillips, 2007). Furthermore, several studies (Abrahams et al., 1995; Zimmermann and Church, 2001; Lee and Ferguson, 2002) have shown that step-pool morphologies tend to maximize flow resistance, leading to minimum velocity and shear stress, which is the final cause of its stability. The maximum flow resistance in step-pool series occurred with significantly shorter spacing than that recommended by soil conservation handbooks for gully control using check dams (Heede, 1976; Morgan, 2005).

Despite all this research, a detailed and systematic definition of the different flow types that might occur in check dam systems for gully restoration has not been found by the authors in the scientific literature. In addition, there is also very little information on how check dam design should take into account either the initial or dam-filling conditions, given that the filling period is highly variable within a specific location due to variable climatic and erosive conditions (Boix-Fayos et al., 2007).

The main aim of this paper is to develop a conceptual model of the hydraulics of check dam systems in straight rectangular gullies in order to establish a theoretical basis for estimating their effectiveness in erosion control. For this purpose, the following specific objectives were considered: (i) to develop a hydraulic conceptual model for describing the range of water profile types that might occur in restored gully reaches, evaluating the efficiency of check dam interventions for initial and dam-filling conditions based on energy balance considerations; (ii) to validate the performance of this model with an accepted hydrodynamic model; (iii) to propose general guidelines for check dam design to optimize the efficiency of the interventions for a broad range of conditions.

2 Methods

2.1 Introduction

The construction of check dams in a gully reach causes a flow perturbation upstream and downstream of each structure. In initial conditions (after construction, when no silting has taken place) it creates a backwater effect by increasing the water depth immediately upstream of the structure, leading to a subcritical regime (Froude number $F < 1$). It also produces a water drop downstream of the check dam, which accelerates the flow leading to supercritical flow conditions ($F > 1$) at the impact zone. The spillway performs as a control section, imposing critical flow conditions ($F = 1$). Since, in a restored reach, subcritical flow conditions exist in the downstream sections and the regime is supercritical in the upper part, a hydraulic jump (hereafter HJ) develops in an intermediate cross section (Fig. 1a).

For dam-filling conditions, a hydraulic jump habitually occurs between the critical flow at the downstream spillway and the supercritical regime at the impact region upstream. In this case, we assumed that the top surface of the sediment wedge was a plane extending from the spillway of the downstream check dam to the toe of the upstream check dam (Fig. 1b).

2.2 Description of the conceptual model

The conceptual model of check dam hydraulics was developed to simulate the main modifications induced by check dam construction in the flow regime along restored reaches. The objectives of the model were to provide a better understanding of the main hydraulic processes involved, to assess the influence of the different regimes on the energy dissipation patterns and, as a result, to inform the decision-making process at the design stage of gully control measures. One of the main priorities was to keep the calculations as simple as possible, while still keeping track of the relevant phenomena. The main simplified assumptions considered were: (a) gully reaches are straight and

present rectangular-shaped cross-sections; (b) the HJ characteristics correspond to their classical form.

The model features a combination of mathematical approximations to the different subprocesses:

- Rand Equations for the impact flow features in straight drop structures.
- Classical hydraulic jump expressions (Vischer and Hager, 1995).
- Free-surface profiles, hereafter FSP, calculations or backwater calculations, according to Chanson (1999).

The model was programmed in a standard spreadsheet implemented in a MS Excel® file and was structured in four interrelated modules (normal flow conditions, impact flow, FSP and HJ features). The lengths associated to rapidly varied flows (i.e. impact and HJ length) were explicitly considered, since their dimensions have a relevant impact on the final FSP and, therefore, on dissipation patterns and overall efficiency.

The main input parameters of the model were:

a. Unitary discharge q ranging from 0.1–1 $m^2 s^{-1}$, the typical span of values for channels, gullies and step-pool reaches (Hager and Vischer, 1995; Zimmerman and Church, 2001; Merrit and Wohl, 2002; Castillo, 2012).

b. Bed slopes ranging from 0.02 to 0.1.

c. Effective height z of the check dam between 0.5–1.5 m.

d. Channel roughness ranging from 0.03 to 0.06, from clean and straight to weedy winding channels (Chow et al., 1994).

The model allowed the determination of the different output variables (flow depth, velocity, shear stress, Froude number, friction slope) on a cross-sectional basis at 0.1 m intervals as well as average values along the reach.

2.2.1 Assessment of normal flow conditions

Uniform open channel flows are characterized by a constant flow depth and mean velocity as well as by a friction slope S_f in equilibrium with bed slope S, and are usually known as normal flows (Chanson, 1999). They represent the starting situation (assuming straight uniform channels) prior to check dam construction and thereby serve as a reference for comparison to evaluate the efficiency of the conservation measures. Moreover, once the intervention has been carried out, normal conditions (hereafter, NC) define the situation to which non-uniform flow regimes tend since it is an equilibrium of the flow with respect to the bed slope.

In rectangular channels in which flow depth d is significantly smaller than channel width w, the hydraulic radius R can be approximated by d. Thus, the Froude number corresponding to normal conditions F_n can be estimated using Manning's expression:

$$F_n = \frac{u}{\sqrt{g\,d_n}} = \frac{\left(\frac{R_n^{2/3}\cdot S^{0.5}}{n}\right)}{\sqrt{g\,d_n}} \approx \frac{\left(\frac{d_n^{2/3}\cdot S^{0.5}}{n}\right)}{\sqrt{g\,d_n}} = \frac{d_n^{1/6}\,S^{0.5}}{n\sqrt{g}} \quad (1)$$

where the subscript n indicates normal conditions for the hydraulic variables, n Manning's roughness coefficient and S the bed slope of the gully.

For a given unitary discharge q, the flow depth d in a rectangular channel can be estimated using Manning's equation and again assuming $R \sim d$:

$$q = u \cdot d \approx \frac{d^{5/3}\cdot S^{0.5}}{n}. \quad (2)$$

Solving this for d_n, we obtain:

$$d_n \approx \left(\frac{n\cdot q}{S^{0.5}}\right)^{3/5}. \quad (3)$$

Finally, using Eqs. (1) and (3), an expression for F_n which is dependent only on primary variables can be calculated:

$$F_n \approx \frac{\left(\frac{n\cdot q}{S^{0.5}}\right)^{1/10} S^{0.5}}{n\sqrt{g}} = \frac{q^{0.1}\cdot S^{0.45}}{n^{0.9}\sqrt{g}} = 0.319\cdot\frac{q^{0.1}\cdot S^{0.45}}{n^{0.9}}. \quad (4)$$

Therefore, F_n, d_n and u_n can be estimated directly from the input parameters q, S and n, allowing the direct determination of the hydraulic regime for NC.

2.2.2 Flow regime at the impact

Rand equations, in the form provided by Chanson (1999), were applied to determine the flow characteristics at the impact:

$$\frac{L_i}{z} = 4.3\left(\frac{d_c}{z}\right)^{0.81} \quad (5)$$

$$\frac{d_i}{z} = 0.54\left(\frac{d_c}{z}\right)^{1.275} \quad (6)$$

where d_c is the critical depth, z the effective height of the check dam, L_i the impact length and d_i the supercritical flow depth at the impact.

2.2.3 Free-surface profile determination

Check dam series simultaneously produce gradually varied flows (GVF), i.e. sub- and super-critical zones along the gully (Fig. 1), and rapid varied flows (RVF), such as HJ and waterfall impact. As a result of these transitions, flow velocity, flow depth and shear stress vary along the channel, and normal conditions (friction slope S_f equalling gully slope S at all sections), are not applicable. The value for each of the hydraulic variables in a particular cross section can be calculated by solving iteratively the continuity and

energy equations following backwater calculation methodology (Chanson, 1999). This approach can be applied to the hydraulic calculations both in subcritical regimes (controlled by backwater conditions) as well as in supercritical flows (governed by upstream controls).

The determination of free-surface profiles (FSP) in a reach controlled by a series of check dams requires hydraulic calculation in both directions, from the lower dam backwards (subcritical regime imposed by the water surface elevation) and from the upper dam forward (supercritical regime after the drop). Within the FSP approach, the step method-depth calculated from distance was applied (Chanson, 1999). This method comprised the following steps: (i) definition of the control sections downstream (at the spillway, where critical conditions are reached) and upstream (where flow characteristics can be estimated at the impact zone); (ii) application of the differential energy equation at 0.1 m intervals in both directions in order to determine the FSP (flow depth) and derivative variables (velocity, friction slope, shear stress) at each cross-section.

2.2.4 Hydraulic jump equations

Classical hydraulic jump expressions (flat rectangular channel), were used to determine the main HJ characteristics, i.e. length of the roller and the amount of dissipated energy H_j (Chanson, 1999). Although the application of these equations on sloping channels (either positive or negative) produces errors in the estimation of the FSP and energy calculations, they provide a valid approximation for the overall conceptual assessment of the flow regimes, while keeping the simplicity of the model implementation.

In the model, the HJ characteristics were estimated by comparing graphically the FSP calculated in both directions in order to find the point of correspondence between the downstream subcritical and upstream supercritical regimes. For this purpose, the Froude numbers at the supercritical zone were transformed to their sequent values considering a longitudinal offset equal to the estimated HJ length. The cross-section at which both curves intersected defined the location of the subcritical section of the HJ and the value of the common Froude number, that is, the subcritical F of the HJ.

2.3 Analysis of the regimes of influence in the hydraulic jump

The hydraulic jump is the most relevant process produced by the hydraulic influence of check dam systems on water flow. Here we use the term *regime of influence* to refer to the control exerted over the HJ characteristics either by the normal conditions in the gully or the check dam downstream.

The regime of influence over the hydraulic jump has been classified following two criteria: (i) the element that exerts the influence; (ii) the level of influence.

i. Element exerting the influence:

1. Normal conditions (NC):
   For initial conditions, the HJ features are controlled by NC (either subcritical or supercritical) when the check dams are at enough distance to avoid dam influence, allowing the establishment of a normal flow.

   For dam-filling conditions, we can assess the modified NC corresponding to the slope of the sediment wedge or deposition slope. The deposition slope S_d (Heede, 1976) can be expressed as a function of the original slope and the geometric factor of influence c:

$$S_d = \frac{L \cdot S - z}{L} = S - \frac{z}{L} = S \cdot \left(1 - \frac{z}{L \cdot S}\right) = S \cdot (1 - c) \quad (7)$$

   where z is the effective check dam height (to the bottom of the spillway), L the check dam spacing in horizontal projection, S the bed slope and c given by:

$$c = \frac{z}{L \cdot S}. \quad (8)$$

   For $c = 1$ the deposition slope is zero, the surface of the sedimentation wedge is horizontal and the bottom spillway elevation of the downstream check dam is the same as the toe elevation of the upstream check dam (head-to-toe rule). For

$c > 1$, the deposition slope S_d is negative. As S_d must be positive to define any normal flow regime, modified NC conditions only can be determined for $c \leq 1$ and, in addition, S_d must remain sufficiently low to achieve subcritical conditions. If S_d did not fulfill this latter requirement, no hydraulic jump will occur and the regime along the reach will remain supercritical.

2. Downstream check dam:
   As for the initial conditions, the HJ location is controlled by the subcritical conditions imposed by the downstream check dam as a consequence of the rise in elevation of the free-surface over the spillway (downstream control). As for the dam-filling conditions, this influence is only exerted for $c \geq 1$. In both cases, the check dam influence dominates over the NC when adjacent check dams are close enough not to allow the development of a normal flow.

ii. Level of influence:
   This classification takes into consideration the dissipation efficiency of the HJ occurring in a controlled reach as a consequence of the control imposed by the tail-water level. Several cases can be considered regarding the level of influence on the HJ:

1. Submergence:
   This phenomenon is characterized by the absence of HJ. In this case, due to the negligible check dam dimensions for a given flow, the structure does not modify the flow regime corresponding to NC. The check dam construction will not produce any impact on the hydraulic regime and the control measure would be inefficient. It corresponds with very slow regimes, high discharges and/or small check dam heights. Normally, the specific energy for NC E_n is below E_i. However, when z is small or the flow discharge high, similar values for E_n and E_i can be obtained. At the limit, if those values were equal, the water free-surface will evolve to NC without the development of a hydraulic jump. This condition defines the submergence threshold:

$$E_n = E_i = E_c + z = 1.5\,d_c + z. \quad (9)$$

   Submergence is not a limiting factor for check dam design in practice, since it would require negligible check dam heights when compared with the scale required for gully restoration and practical considerations: less than 0.4 m in all cases and around 0.1 m for F_n values in the proximity of 0.6 (typical of slow-flow conditions such as weedy downstream reaches close to the gully mouth).

2. Partial hydraulic influence (PI):
   We named partial hydraulic influence (PI) that situation in which HJ occurs at a certain distance from the check dam toe and, therefore, the supercritical Froude number of the HJ (F_1) downstream of the check dam is smaller than the Froude number at the impact F_i. Thus, the dissipation efficiency of the HJ is below the maximum.

3. Total hydraulic influence (TI):
   The influence will be total (TI) when the HJ takes place immediately after the impact, where all the energy provided by the drop is employed to enhance the HJ performance and $F_i = F_1$.

4. Submerged jump:
   The subcritical Froude number defined by the tail-water level at the toe of the upstream check dam is smaller than the sequent Froude number of F_i. Thus, the hydraulic jump is submerged, producing a dissipation efficiency lower than TI conditions (Vischer and Hager, 1995).

The hydraulic influence differs from the geometric influence determined by c, since the former refers to the dissipation performance of the HJ, whereas the latter expresses merely a geometric relationship. Partial hydraulic conditions occur when $c \ll 1$ and total influence is usually produced when $c \sim 1$ or even $c > 1$. While the geometric influence

is straightforward to determine, the hydraulic influence requires the solution of RVF and FSP using a hydraulic model.

2.4 An energy-based approach to assessing the efficiency of check dam interventions

In this study, a new methodology is proposed to estimate the performance of the check dam construction when compared with a non-intervention scenario based on energy considerations (Fig. 2).

The difference in total head between adjacent check dams corresponds to the $L \cdot S$ product. In a gully without intervention, this energy is dissipated completely through bed friction ($H_{\text{dis-NC}}$) at the wetted perimeter of the cross section at a rate given by the NC regime. Assuming uniform flow, this energy can be expressed as a function of hydraulic and geometric variables:

$$H = L \cdot S = H_{\text{dis-CN}} = \frac{L \cdot \tau_{\text{n}}}{\gamma \cdot R_{\text{n}}} \tag{10}$$

where τ_{n} is the shear stress for normal conditions (NC) in Pa, R_{n} the hydraulic radius for NC in m and γ the water specific-weight in $N \cdot m^{-3}$. Therefore, all the energy needs to be dissipated by exerting a drag tension over the gully bed. In this case, the friction slope is equal to the bed slope ($S_{\text{f}} = S$) at all the cross-sections.

In contrast, after the check dam construction, energy losses appear at the impact zone (H_{i}) and at the hydraulic jump (H_{j}), reducing the dissipation through bed friction (H_{dis}):

$$H = L \cdot S = H_{\text{i}} + H_{\text{j}} + \sum H_{\text{dis}} \tag{11}$$

$$\sum H_{\text{dis}} = L \cdot S - \left(H_{\text{i}} + H_{\text{j}}\right) = L \cdot S_{\text{fm}} = \frac{L \cdot \tau_{\text{m}}}{\gamma \cdot R_{\text{m}}} \tag{12}$$

where $S_{\text{fm}}$is the mean friction slope, τ_{m} is the mean shear stress and R_{m} the mean hydraulic radius in the controlled reach.

Since $\sum H_{\text{dis}} < H_{\text{dis-NC}}$, the mean values of the hydraulic variables responsible for the erosion processes (e.g. S_{fm} and τ_{m}) are reduced in the post-intervention scenario at the expense of creating local energy losses at particular locations. If this dissipation occurs under non-protected conditions, an intensification of the erosive processes might take place.

The average slope friction S_{fm} at the corrected reach was calculated according to Eq. (13):

$$S_{\text{fm}} = \frac{\sum H_{\text{dis}}}{L} = \frac{L \cdot S - \left(H_{\text{i}} + H_{\text{j}}\right)}{L} = S - \frac{H_{\text{i}} + H_{\text{j}}}{L}. \tag{13}$$

The energy losses at the impact zone were estimated using Eq. (14):

$$H_{\text{i}} = (E_{\text{c}} + z) - E_{\text{i}} = (1.5\, d_{\text{c}} + z) - \left(d_{\text{i}} + \frac{u_{\text{i}}^2}{2\,g}\right) \tag{14}$$

where E_{c} is the specific energy for critical depth over the spillway and E_{i}, d_{i} and u_{i} are the specific energy, flow depth and velocity at the impact zone, respectively. The flow characteristics at the impact zone were estimated using Eq. (6).

The energy losses at the hydraulic jump H_{j} were estimated assuming a classical HJ. For HJ submergence conditions, the total energy dissipation $H_{\text{t}} = H_{\text{i}} + H_{\text{j}}$ was estimated as the difference of total heads between the critical regime at the spillway ($E_{\text{c}} + z$) and the subcritical conditions imposed by tail-water level at the impact length L_{i} due to the difficulties inherent in calculating H_{i} and H_{j} separately for such a complex hydraulic regime.

The efficiency of a check dam intervention was defined as the percentage of reduction of the mean value of the friction slope S_{fm} at the corrected reach when compared to the friction slope value for NC prior to the intervention ($S_{\text{fm}} = S$). The efficiency in reduction of friction slope E_{s} can be directly calculated using Eq. (15):

$$E_{\text{s}} = \frac{S - S_{\text{fm}}}{S} \cdot 100 = \frac{H_{\text{i}} + H_{\text{j}}}{L \cdot S} \cdot 100. \tag{15}$$

2.5 Methodology for analyzing check dam systems

2.5.1 Determining the hydraulic regime for normal conditions

The areas of occurrence for sub- and supercritical regimes in normal conditions were assessed as a function of the unitary discharge, bed slope and roughness in order to evaluate the conditions in which they appear in gully networks (Eq. 4).

2.5.2 Classifying free-surface profiles

We have classified the different flow regimes that might occur in a restored reach using four indices: (a) silting of the check dams: initial or dam-filling conditions; (b) Froude regime for NC: subcritical or supercritical; (c) element controlling the HJ; (d) level of influence.

2.5.3 Contrasting the model

To validate the conceptual model, we compared the performance of the model against the results provided by the hydrodynamic bi-dimensional IBER model v1.9 (GEAMA, Instituto Flumen and CIMNE, Spain). IBER is free-to-use software for flow simulation applications featuring a hydrodynamic module based on 2D-Saint-Venant equations and a finite-volume method used for the characterization of unsteady flows and hydraulic jump formations.

The procedure for obtaining the IBER simulation was as follows: (i) definition of the geometry as a triangulated irregular network of 0.1 m cells; (ii) definition of the initial and boundary conditions; (iii) creation of the model mesh for the mathematical calculations; (iv) definition of channel roughness; (v) calculations and extraction of results as graphics (e.g. Froude number longitudinal profiles). The 3-D input geometry reproducing the initial and dam-filling channel geometry was obtained using Matlab® scripts

(The MathWorks™ Inc., Natick, MA, USA) specifically designed by the authors for this purpose.

2.5.4 Evaluating check dam efficiency

An analysis of the main factors of influence on check dam efficiency (unitary discharge, check dam height, bed slope and roughness) was carried out. This study was conducted by executing the model with increasing c in order to characterize the efficiency for a representative sample of the different types of regime described in Sect. 2.5.2. The mean friction slope along the reach was calculated by averaging the S_f between all cross-sections (0.1 m apart) and, also, by applying Eq. (13) and, finally, the efficiency was estimated using Eq. (15).

Additionally, the regions of validity for optimal c over a q, S coordinate system were determined for medium to high roughness conditions to provide practical guidelines for the design of check dam interventions. The optimal c, i.e. value of the geometric factor of influence defining maximum efficiency, was obtained through several trial runs of the model until total influence conditions were achieved for each particular set of conditions (q, S, z, n). In order to design the effective height of the check dam z, a Froude number at the impact region $F_i = 4.5$ was fixed, the threshold value to achieve stable and efficient HJ (Chanson, 1999).

3 Results

3.1 Normal conditions and Froude regime

Figure 3 shows the region where sub- and supercritical flows occur in normal conditions. Supercritical flow is the predominant regime, while subcritical flow only occurs on low slopes (usually below 5 %). In addition, high hydraulic roughness or low discharges induce lower regimes and thereby promote subcritical flows.

3.2 Classifying free-surface water profiles

Figure 4 includes a graphical depiction of the different FSP types that may develop in a gully restoration. For initial conditions, the HJ occurrence is guaranteed as a consequence of the elevation of the water profile behind the downstream check dam, provided that submergence conditions are not verified (IN-SUB-SUM). The location of the HJ is dependent on the element exerting the influence. Thus, if the NC are subcritical, a HJ will occur close to the impact region as soon as the flow has dissipated the excess energy and has reached the supercritical sequent depth corresponding to the subcritical depth associated with that NC (IN-SUB-NC-PI). If the NC were subcritical enough to reach the sequent depth of the impact flow, the HJ would take place at the toe of the check dam (IN-SUB-NC-TI). Thus, total influence is achieved, leading to maximum performance of the HJ. Finally, downstream control by dam influence can only begin when the adjacent dams are close enough to dominate over the NC (IN-SUB-D-PI and IN-SUB-D-TI).

Supercritical NC lead to an undesirable uncertainty in the location of the HJ, since this occurs at that point where the downstream check dam produces the subcritical control (IN-SUP-NC-PI). The length of the subcritical zone can be estimated, as a first approximation, without doing the FSP calculations, by drawing a horizontal line from the spillway to the bed slope. The HJ occurs when the subcritical regime reaches the sequent depth of supercritical NC.

As for the dam-filling situation, the value of the deposition slope S_d is the key factor determining the type of regime which develops, since it controls the Froude regime associated with the modified NC. If the modified NC are supercritical, a HJ will not take place since there is no downstream control to cause it (F-SUP-NHJ). Therefore, it is necessary for S_d to remain sufficiently low to create subcritical conditions (F-SUB-PI). Nevertheless, in some cases, this condition might not be sufficient to guarantee the effective transition to subcritical flow, since, in terms of energy, the flow requires a certain length to evolve from the supercritical flow at the impact. Depending on the

channel characteristics (q, S and n are input factors) and the design of the intervention (z and c mainly, which define S_d) for an HJ to occur may require horizontal or even negative S_d (F-D-PI and F-D-TI) to be established.

3.3 Contrasting the model

The results of the comparison between the model and IBER for a representative sample of contrasting types of FSP are shown in Fig. 5. These curves represent the spatial evolution of the Froude number F of the flow along the restored reach as predicted by the conceptual model and by IBER. In the same figure, the constant F corresponding to NC (for the initial situation) and also modified NC (for a dam-filling scenario) are shown, in order to understand FSP evolution better.

Overall, the model performed well, producing comparable results with IBER. The curves are mostly coincident especially with regard to the subcritical region, but also, importantly, in the values of F at the HJ in the supercritical region. On the other hand, there are deviations with respect to the F_i at the impact zone and the location of the HJ. Higher HJ and impact lengths were predicted with our model, explaining the visible offsets between both curves at the supercritical region. The biggest differences in check dam efficiency occur when the conceptual model overestimates the Froude number at the impact (IN-SUP-CN-PI and IN-SUP-D-PI), leading to an underestimation of efficiency by the conceptual model (22.3 % instead of 36.6 % and 28.2 % against 44.1 %).

3.4 Assessing the influence of key factors on check dam efficiency

Figure 6 shows a sample of efficiency curves as a function of c, varying one key factor at a time (q, z, S and n). As for initial conditions (Fig. 6a to d), the efficiency curves present an irregular sigmoid shape typically featuring a linear segment at low c, a parabolic segment in the middle and an asymptotic maximum at the highest c values.

The influence of the key factors was noticeable mainly on the maximum level of efficiency and the location of the turning points. Thus, increasing unitary discharges produced lower maximum efficiencies and a displacement of the maximum efficiency in the direction of decreasing c (Fig. 6a). The main impact of higher z was to increase the maximum efficiency and displace it towards increasing c (Fig. 6b). High slopes produced a displacement of the curve to lower c and smaller maximum efficiencies (Fig. 6c), whereas there was little difference between the hydraulic roughness results (Fig. 6d). In all cases, the maximum efficiency took place around $c = 1$.

For dam-filling conditions (Fig. 6e–h), only cases where HJ occurred were considered. Therefore, relatively high values, $c > 0.8$, are presented. Here, it was apparent that, although a general sigmoid shape was found, the curves were more irregular. It is worth noting that in most cases, the curve maximums moved towards $c > 1$ when compared with the initial conditions curves. Those cases corresponding to short spacing between adjacent check dams, either low dam heights z or high slopes S, presented a poorer efficiency performance, with no clear maximums (Fig. 6f and g). Higher z and lower q led to the displacement of the curve maximum in the direction of decreasing c, but in most cases they had little impact on the efficiency value (Fig 6e and 6f). An intermediate slope produced the highest maximum efficiency at the expense of higher c (Fig. 6g). Finally, a higher roughness coefficient required smaller c to reach the maximum and the efficiency was slightly lower (Fig. 6h).

Considering all the cases included in the above analysis, the relationship between the efficiency obtained by averaging S_f at 0.1 m intervals and calculating S_f using Eq. (13) rendered the linear regression $E_{s\text{-}Eq.13} = 1.01 \cdot E_{s\text{-}0.1m}$ and $R^2 = 0.99$ for $n = 72$. Thus, the combination of Eqs. (13) and (15) represented a straightforward way to estimate the performance if H_i and H_j were easily known, as in the case of total influence.

Overall, it was clear that in both situations (initial and dam-filling conditions) high maximum efficiencies were achieved, slightly lower in the former case (> 80 %) than in the latter (> 90 %), although for initial conditions, the location of the maximum took place at lower c, that is, at a larger spacing. Those high efficiencies will result in a significant decrease in the final average friction slope S_{fm}, from a five- to ten-fold reduction of the original slope, leading to a S_{fm} below 2 %. In most situations, this large drop in the friction slope is likely to be enough to reduce shear stresses below the threshold of erosive processes.

To provide a better understanding of the processes involved, Fig. 7 shows the evolution of the main energy parameters with increasing c for initial conditions. As the check dams get closer, the difference in total head between adjacent dams (LS) decreases. Energy losses at the impact H_i are constant, as calculated using Eq. (14). The dissipation of energy at the hydraulic jump is minimum throughout the NC-influence segment (in this case $c = 0.7$, the NC flow supercritical and $F_1 = F_n = 1.4$ producing poor HJ performance) and starts to grow as the dam influence begins to operate. The higher the dam influence, the lower the subcritical flow at tail-water level, enhancing the HJ performance. When total influence is achieved (subcritical tail-water level reaches the sequent value of F_i) H_j and, therefore, the total energy losses at dissipation phenomena H_t, are maximum. At shorter spacings, the HJ becomes submerged and loses efficiency, causing a decrease in H_t.

3.5 Regions of optimal *c*

Figure 8 illustrates the procedure employed to determine the regions of optimal c (i.e. total influence condition and maximum efficiency) valid for both initial and dam-filling conditions.

Firstly, the curves of optimal c were calculated for initial conditions using the model and considering a range of situations with q and S as input variables (z was calculated using $F_i = 4.5$ criterion which is only dependent on q). In this case (dotted lines in Fig. 8a), the curve of optimal c represents a floor-type threshold, i.e. the points above the line verify the condition. For instance, the upper dotted line corresponds to $c = 1$ and q, S conditions above this line verify an optimum efficiency for $c \leq 1$. This floor-type threshold behaviour is a consequence of the influence of the HJ and impact length on the optimal spacing. If their length is negligible, total influence is typically

achieved when $c \sim 1.2$. However, since both processes need space to develop, they push adjacent check dams further away leading to smaller optimal c. The length of the RVF (typically around one or two meters) had a strong impact on c as long as the slope remained high. Figure 8 shows how, as the slopes decreased, c got closer to 1.2 since the RVF lengths were comparatively small compared to the check dam spacing, and their influence was barely noticeable.

Secondly, similarly to the former analysis, curves of optimal c were obtained for dam-filling conditions (solid lines in Fig. 8b). Conversely, the geometric places for optimum efficiencies delimited a ceiling-type threshold, i.e. the points below the line verify the condition. For example, the upper lines correspond to $c = 1$ and the q, S points below it verify the optimal condition for $c < 1$. In this case, the way in which the flow is controlled is through the deposition slope and the spacing between check dams. Dam-filling conditions commonly require negative S_d to achieve total influence, but also enough distance to develop the required subcritical flow corresponding to the Froude number at the impact. Consequently, low slopes (large distances) and small discharges (easier to control since their Froude number and energy evolves faster for the same distance) led to smaller c.

The optimal curves were much more sensitive to roughness in the dam-filling scenario (see the movement upwards of the optimal curves when the roughness increases from Fig. 8a and b), whereas in the initial conditions, the thresholds remained almost unchanged.

Finally, the area enclosed between two of these optimal curves for the same c defined a region of optimal control valid throughout the lifetime of the structure. The more intensive the control exerted (higher c), the larger the region of validity of the design. These results are shown in Figure 9, representing the regions obtained on a $S - q$ plane verifying simultaneously the condition of optimal c for initial and dam-filling situations for two different roughness coefficients: $n = 0.04$ (clean, winding channels) and $n = 0.06$ (winding channels with weeds and pools).

Figure 9a shows that the total geometric influence $c = 1$ was not valid to create optimal efficiencies along clean channels ($n = 0.04$), since its region of validity was negligible (small black triangle). Values up to 1.2 would be necessary to cover the range of slope and unitary discharge defined. However, if a channel is covered with vegetation ($n = 0.06$, Fig. 9b), there is a significant area (up to 9 % of slope and 0.5 $m^2 s^{-1}$ discharge) that reaches optimal efficiencies for $c = 1$. Only for high unitary discharge or steep slopes would c values above 1 be required.

4 Discussion

4.1 Erosion implications of the typologies of flow regimes

The study of the Froude regime for NC showed that supercritical flows are predominant in gullies defined by erosion surfaces with scarce vegetation and steep slopes. These rapid supercritical flows are associated with high shear stress and friction slope values, which are the final cause of the erosion processes that lead to the development and growth of gully networks. Their spatial extent is only controlled by the backwater effect of the downstream dam, so that, if c is low, a large part of the gully remains under supercritical conditions.

If this happens, the new situation is more erosive than that prior to the intervention since the waterfall at the check dam produces an accelerated flow more intense than the former situation until it evolves to NC. This fact is illustrated in Fig. 5: F above the NC line indicates more erosive power than the non-intervention scenario and F below, less erosive conditions. In addition, HJ occurs at an intermediate, unprotected section of the reach favouring further degradation processes. Both reasons contribute to the scouring processes reported in many check dam works, which may ultimately lead to the complete destruction of the structure. Consequently, badly designed check dam structures might in fact be more harmful than non-intervention (Heede, 1978).

The response in check dam efficiency results from the ratio of dissipated energy and decreasing total available energy LS, as illustrated in Fig. 10. Along the NC-influence segment, the growth is linear since H_t remains constant but LS decreases. The parabolic shape (dam-influence conditions) stems from both the reduction of LS and the increase of H_j losses. The total influence defines maximum efficiency (maximum H_t and low LS) which is maintained for higher c since the reduction in LS compensates for the decrease in H_t.

Achieving total influence is recommended both for efficiency in the reduction of erosive power, as well as for protection of the check dam system. Total influence implies maximum dissipation losses located at the toe of the check dam (around 90 % of the total head), where a protective apron must be set. As a result, a slow subcritical flow with low erosive power will develop along the rest of the gully, hindering the activation of new stages of degradation.

For higher q and S but lower z, the check dam spacing must be reduced, while increasing roughness has the opposite effect, allowing an increase of the spacing between check dams. A suitable choice is to adapt the dam height z to the q to be controlled, and this effect is achieved if a minimum F_i is fixed with respect to HJ stability ($F_i = 4.5$). The vegetation of the gully sides, a common practice used to increase slope stability against bank failure, has the additional positive side effect of moving the system into a more stable stage since it increases hydraulic roughness, especially in dam-filling conditions.

4.2 Validity of the model

Although the hypothesis underlying its definition led to major simplifications (rectangular gullies, classical HJ), the simplicity of the calculations enabled us to focus on the concepts and an overall understanding of the hydraulics, which may not have been possible using more sophisticated tools.

The contrast with the simulations performed by the IBER model was satisfactory both in the longitudinal hydraulic profiles and in overall efficiency. This suggests that

our model can be applied with confidence for a general assessment of free-surface profiles. The discrepancies found in the estimation of RVF lengths and efficiency were expected, due to the complexity of modelling these processes and the sensitivity of FSP to the length of the impact and HJ with the short spacing derived from keeping c in the proximity of 1.

Although the model proved to be successful in providing insight into the key processes involved in gully control, it does not account for many phenomena occurring in more realistic situations such as those derived from local slope changes, meanders, presence of pools, stones and weeds, erosion and sedimentation dynamics, all of which may have a strong impact on flow characteristics. For instance, Polyakov et al. (2013) reported partial burying at the downstream part of check dams, a fact which departs from the assumed spillway-to-toe hypothesis for a plane sediment wedge. Further studies should undertake more sophisticated hydraulic analysis, combined with observation of check dam systems under field conditions, to improve our understanding of the modifications produced by check dam measures in complex channel morphologies.

4.3 Practical guidelines for check dam design

As for effective height definition, the $F = 4.5$ criterion is recommended, which is the threshold for stable HJ without creating an excessively powerful waterfall prone to cause scouring. When this criterion is applied, z can be estimated using a function of q:

$$z = 1.9 \cdot q^{0.67}. \quad (16)$$

For $q = 1\,m^2\,s^{-1}$, z will remain lower than 2 m. However, values of q between 0.3–$0.5\,m^2\,s^{-1}$ are recommended, resulting in a z value around 1m, which are suitable dimensions for constructing simple, inexpensive check dams in agricultural areas using the farmer's own means. In this respect, the width of the spillway can be selected to attain the target q, provided that the gully bed is at least the same width to avoid scouring the banks.

Furthermore, the combination of a check dam construction along with vegetation is highly recommendable, not only because the additional protection that plant cover provides the banks, but also because it increases the hydraulic roughness leading to lower optimal c. In fact, $c = 1$ criterion is recommended, since it provides the interventions with optimal efficiency in most gully conditions, while representing a straightforward rule for check dam spacing in the field (head-to-toe rule applicable with a simple water level). If steeper reaches are considered (20 % or more), alternative ways of dissipating the excess energy of the flow should be explored, since restoration of the check dam might be costly and inefficient.

Despite the fact that authors such as Heede (1978) have proposed using empirical rules to determine the ultimate slope of sediment deposits as a function of the original bed slope (e.g. a ratio of 0.28 between slopes and thereby $c = 0.72$ for Alcali Creek watershed) in order to avoid overdesign, our findings suggest that shorter spacings are required to provide effective control. Thus, it would be preferable to increase the cost constructions by 30 % ($c = 1$ criterion) to operate with a wider safety margin, taking into account the real risk of undercutting and reactivation of gully erosion with eventual high discharges, which is bound to happen during the expected lifetime of the structures (usually 25 yr).

One main drawback of the ultimate slope criterion is its assumption of the development of a uniform regime when the ultimate slope is achieved in filling conditions, a situation which is not applicable in restored reaches characterised by highly non-uniform regimes. Furthermore, the relatively small diameter of soil particle size of gully sediments in agricultural areas (in contrast with steep mountain reaches where cobbles and boulders might be predominant) will probably lead to gentle, almost horizontal slopes to keep the bed shear stresses below the critical value. Thus, the previous consideration regarding the suitability of the $c = 1$ criterion can also be valid in this case.

The occurrence of maximum efficiencies at an optimal c has remarkable similarities with the maximum resistance principle formulated by Abrahams et al. (1995) for step-pool streams. In their study, the $\frac{H}{LS}$ index was defined as the key variable controlling

resistance and, later, this parameter was named as steepness factor c (Lenzi and Comiti, 2003). Its definition is almost identical to geometrical influence factor c, but for the numerator H, which could be affected by the deposition or, more frequently, the scouring beneath the step. In natural step-pool streams, $\frac{H}{LS}$ values typically ranged between 1 and 2. The optimal c values obtained in this study for dam-filling situations fell within this interval, with values around 1.5 or above when high slopes or small heights were considered (Fig. 6f and g), i.e. when short spacing between adjacent dams were considered. These assumptions might be applicable to step-pools, since they are steep streams with step heights limited by the available boulder size.

If this hypothetical analogy is valid, it will provide an interesting parallel between man-made interventions and natural self-organized streams, pointing out the necessity of imitating nature to ensure the stability of the intervention in the long-term. It will also reinforce our conclusions regarding the need to design check dam locations following the geometric total influence criterion.

5 Conclusions

The model has combined in a single framework different previous approaches related to hydraulic processes occurring in restored channels to explain the basic flow modifications that check dams produce. Its comparison with the hydrodynamic IBER model produced comparable results, although some differences in the hydraulic jump and impact lengths were found. Among all the possible regimes, total influence is the only situation in which the dissipation efficiency is maximised (effectiveness requirement) and the HJ is also forced to occur at the toe of the structure (security requirement). Under high roughness conditions (either natural or induced by revegetation), the total geometric influence ($c = 1$) turned out to be a suitable criterion to reach optimal control at the different filling stages of the structures as well as a convenient rule for dam location in the field. The maximisation of energy dissipation by total influence presents similarities with the maximum resistance principle formulated by Abrahams et al. (1995) for

step-pool streams, which suggests there is a close bond between naturally developed systems and man-made interventions.

Acknowledgements. This study was supported by Projects P08-AGR-03925 (Andalusian Government), AGL2009-12936-C03-01 (Spanish Ministry of Science and Innovation), AGL2012-40128-C03-01 (Spanish Ministry of Economy and Competitiveness), RESEL (Spanish Ministry for Environment and Rural and Marine Affairs) and FEDER funds. This support is gratefully acknowledged.

References

Abrahams, A. D., Li, G., and Atkinson, J. F.: Step–pool streams: adjustment to maximum flow resistance, Water Resour. Res., 31, 2593–2602, 1995.

Boix-Fayos, C., Barberá, G. G., López-Bermúdez, F., and Castillo, V. M.: Effects of check-dams, reforestation and land use changes on river channel morphology: study case of the Rogativa catchment (Murcia, Spain), Geomorphology, 91, 103–123, 2007.

Castillo, C.: Metodología de medida de la erosión por cárcavas y modelado de su control mediante diques de retención, PhD Thesis, University of Córdoba, 2012.

Castillo, V. M., Mosch, W., Conesa García, C., Barberá, G. G., Navarro Cano, J. A., and López-Bermúdez, F.: Effectiveness and geomorphological impacts of check dams for soil erosion control in a semiarid Mediterranean catchment: El Cárcavo (Murcia, Spain), Catena, 70, 416–427, 2007.

Chanson, H.: The Hydraulics of Open Channel Flow: An Introduction, Butterworth-Heinemann, Oxford, UK, 512 pp., 1999.

Chin, A. and Phillips, J. D.: The self-organization of step-pools in mountain streams, Geomorphology, 83, 346–358, 2007.

Chin, A., Anderson, S., Collison, A., Ellis-Sugai, B., Haltiner, J., Hogervorst, J., Kondolf, G. M., O'Hirok, L. S., Purcell, A. H., Riley, A. L., and Wohl, E.: Linking theory and practice for restoration of step-pool streams, Environ. Manage., 43, 645–661, 2009.

Chow, V. T., Maidment, D. R., and Mays, L. W.: Hidrología Aplicada, McGraw-Hill Interamericana S.A., Santafé de Bogotá, Colombia, 1994.

Conesa-García, C., López Bermúdez, F., and García-Lorenzo, R.: Bed stability variations after check dam construction in torrential channels (South-East Spain), Earth Surf. Proc. Land., 32, 2165–2184, 2007.

GEAMA: Instituto Flumen and CIMNE: IBER model v.1.9, available at http://www.iberaula.es/web/index.php, last access: 5 June 2012.

Heede, B. H.: Early gully-control structures in the Colorado Front Range, Station Paper no. 55, Forest Service, USDA, Fort Collins, Colorado, 1960.

Heede, B. H.: Gully development and control: the status of our knowledge, Research paper RM 169, Forest Service, USDA, Fort Collins, Colorado, 1976.

Heede, B. H.: Designing gully control systems for eroding watersheds, Environ. Manage., 6, 509–522, 1978.

Iroume, A.: Corrección de los cauces torrenciales del Cerro Divisadero, Chile, Bosque, 17, 65–81, 1996.

Iroume, A. and Gayoso, J.: Evaluación de obras y sistemas de corrección de torrentes del cerro Divisadero, Coyhaique, Chile, Bosque, 12, 27–35, 1991.

Lee, A. J. and Ferguson, R. I.: Velocity and flow resistance in step-pool streams, Geomorphology, 46, 59–71, 2002.

Lenzi, M. A.: Stream bed stabilization using boulder check dams that mimic step-pool morphology features in Northern Italy, Geomorphology, 45, 243–260, 2002.

Lenzi, M. A. and Comiti, F.: Local scouring and morphological adjustments in steep channels with check-dam sequences, Geomorphology, 55, 97–109, 2003.

Merritt, D. M. and Wohl, E.: Downstream hydraulic geometry and channel adjustment during a flood along an ephemeral, arid-region drainage, Geomorphology, 52, 165–180, 2003.

Milzow, C.: The step-pool morphology of a steep mountain stream, Diploma thesis. ETH, Eidgenössische Technische Hochschule Zürich, Institut für Hydrologie und Wasserwirtschaft, Zürich, 2004.

Morgan, R. P. C.: Soil Erosion and Conservation, 3rd Edn., Blackwell Publishing, Cornwall, UK, 2005.

Nyssen, J., Veyret-Picot, M., Poesen, J., Moeyersons, J., Haile, M., Deckers, J., and Govers, G.: The effectiveness of loose rock check dams for gully control in Tigray, northern Ethiopia, Soil Use Manage., 20, 55–64, 2004.

Polyakov, V. O., Nichols, M. H., McClaran, M. P., and Nearing, M. A.: Effect of check dams on runoff, sediment yield and retention on small semi-arid watersheds, in review, 2013.

Porto, P. and Gessler, J.: Ultimate Bed Slope in Calabrian Streams Upstream of Check Dams: Field Study, J. Hydraul. Eng., 125, 1231–1242, 1999.

Vischer, D. L. and Hager, W. H.: Energy dissipators, IAHR, AA Balkema, Rotterdam, the Netherlands, 1995.

Wang, Z. Y. and Yu, G. A.: Step-pool system for erosion control and ecological restoration, Keynote Paper, in: Proc. of International Conference on Erosion and Torrential Control as a Factor in Sustainable River Basin Management, Belgrade, Serbia, 1–17, 2007.

Weinhold, M.: The Alkali Creek Story: 40 Years of Gully Control, Proceedings of the Forest Service National Earth Sciences Conference, 18–22 October 2004, San Diego, CA, PNWGTR-689, Department of Agriculture, Forest Service, Pacific Northwest Research Station, Portland, USA, 2007.

Zimmermann, A. and Church, M.: Channel morphology, gradient profiles and bed stresses during flood in a step-pool channel, Geomorphology, 40, 311–327, 2001.

Table A1. Abbreviations.

d_c	critical depth
d_n	normal depth
d_1	supercritical depth at the hydraulic jump
d_2	subcritical depth at the hydraulic jump
D	check dam influence
E_{fs}	efficiency in the reduction of friction slope
Ef_{so}	check dam efficiency predicted in IBER
Ef_{sp}	check dam efficiency predicted by the model
F	dam-filling conditions
F_n	Froude number in normal conditions
FSP	free-surface water profiles
H_{dis1}	energy dissipated due to bed friction in the supercritical region, varied flow conditions
H_{dis2}	energy dissipated due to bed friction in the supercritical region, normal conditions
H_{dis3}	energy dissipated due to bed friction in the subcritical region
H_i	energy dissipated at the impact zone
H_j	energy dissipated at the hydraulic jump
H_t	total energy dissipated ($H_i + H_j$)
HJ	hydraulic jump
IN	initial conditions
L:	check dam spacing
LS	difference in total head between adjacent dams
n	Manning roughness coefficient
NC	normal conditions
NHJ	no hydraulic jump
PI	partial influence
q	unitary discharge
S	bed slope
S_{fm}	average friction slope
SUB	subcritical normal conditions
SUP	supercritical normal conditions
TI	Total influence
u_n	flow velocity in normal conditions
z	effective check dam height

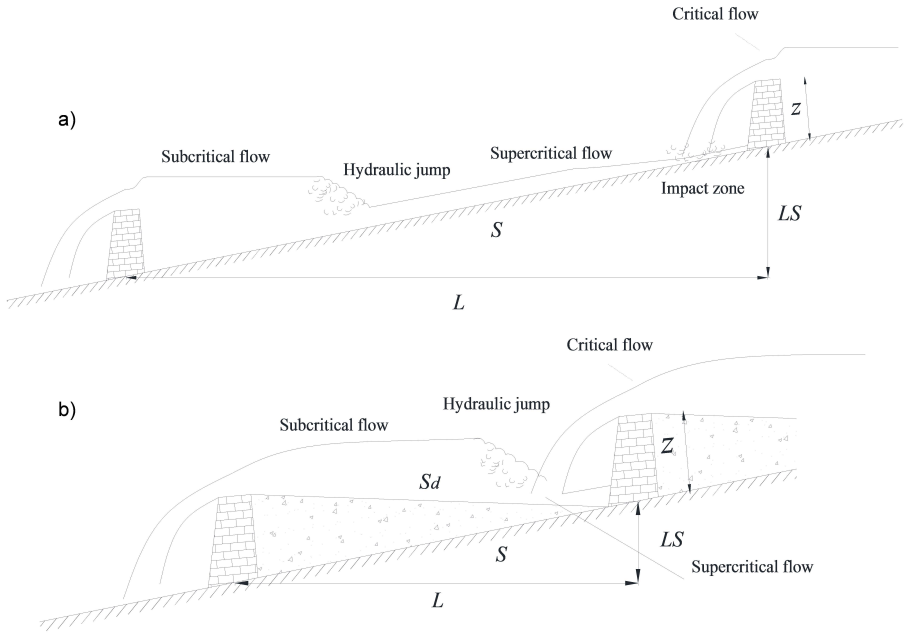

Fig. 1. Sketch of the main hydraulic features and geometric variables after check dam construction, **(a)** initial conditions; **(b)** dam-filling situation. L = spacing between adjacent check dams; LS = difference in elevation between check dams; S = gully slope; S_d = deposition slope; z = effective height of the check dam.

$$H = L \cdot S = H_i + H_j + \sum H_{dis}$$

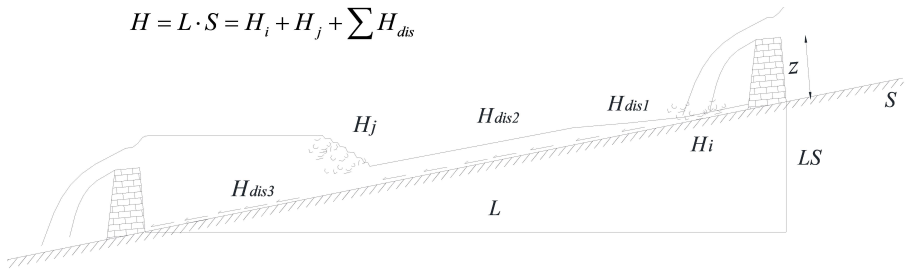

Fig. 2. Energy balance in a controlled gully reach with supercritical normal conditions. H_i = energy dissipated at the impact zone; H_{dis1} = energy dissipated due to bed friction at the supercritical region, varied flow conditions; H_{dis2} = energy dissipated due to bed friction at the supercritical region, normal conditions; H_{dis3} = energy dissipated due to bed friction at the subcritical region; H_j = energy dissipated at the hydraulic jump; S: bed slope; L: check dam spacing; $L \cdot S$ = difference of total head between adjacent check dams; z = effective check dam height.

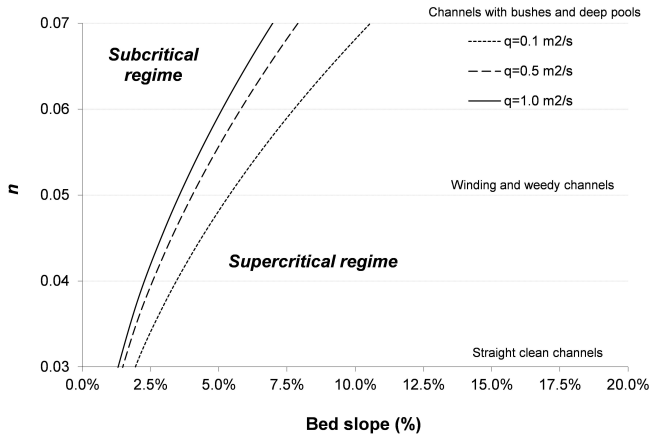

Fig. 3. Froude regime for normal conditions as a function of the unitary discharge q, bed slope S and n Manning roughness coefficient. Grey lines and associated text correspond to different roughness conditions.

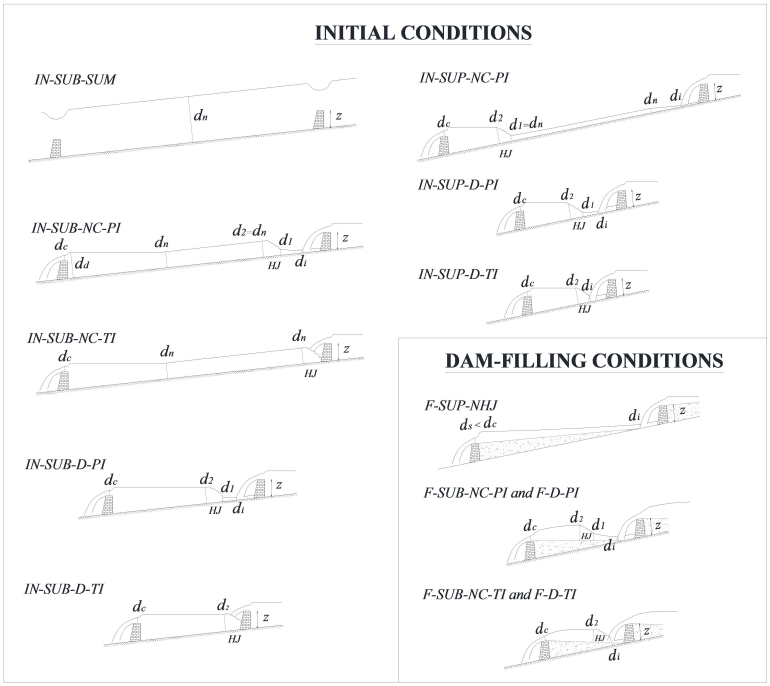

Fig. 4. Classifications of free-surface water profiles in restored gullies. d_c = critical depth; d_n = normal depth; d_s = depth over the spillway; d_1 = supercritical depth at the hydraulic jump; d_2 = subcritical depth at the hydraulic jump; D = check dam influence; F = dam-filling conditions; IN = initial conditions (no deposition); NC = normal conditions influence; NHJ = no hydraulic jump; PI = partial influence; SUB = subcritical normal conditions; SUP = supercritical normal conditions; TI = total influence.

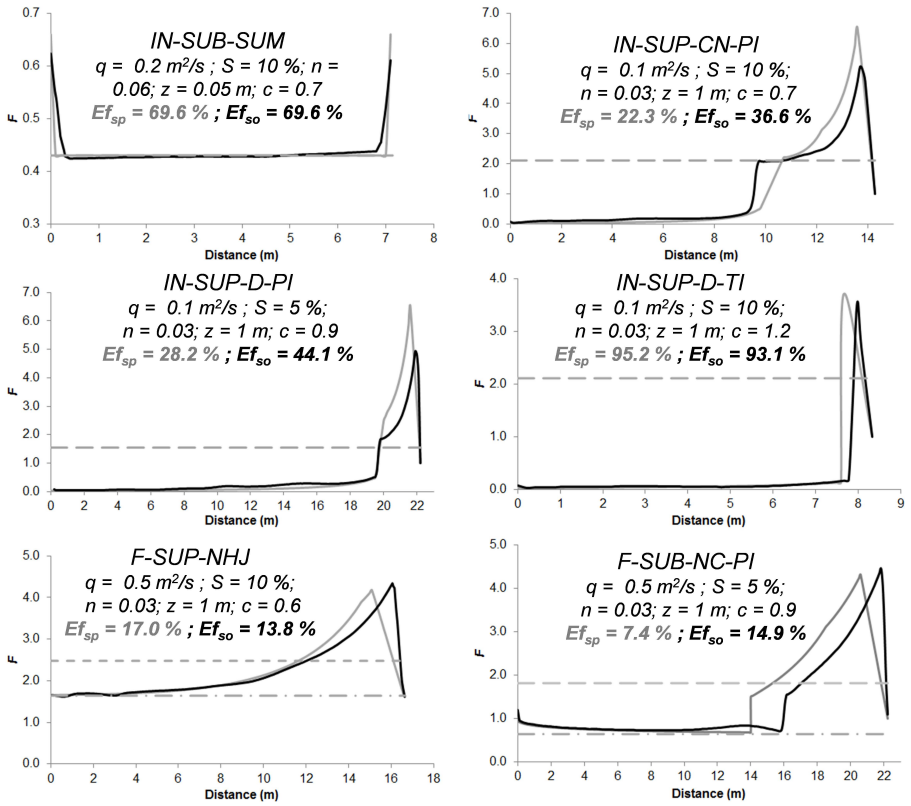

Fig. 5. Comparison of Froude number *F* curves between the model and IBER for different free-surface water profiles types as a function of the distance from the downstream check dam. Solid black lines correspond to predicted results by IBER, solid grey line to predicted results by the conceptual model, the grey dashed line to normal conditions and dashed-dotted line to modified normal conditions for a dam-filling scenario. *D* = check dam influence; Ef_{so} = check dam efficiency predicted in IBER; Ef_{sp} = check dam efficiency predicted by the model; *F* = dam-filling conditions; IN = initial conditions; NC = normal conditions influence; NHJ = no hydraulic jump; PI = partial influence; SUB = subcritical normal conditions; SUP = supercritical normal conditions; TI = total influence.

Discussion Paper | Discussion Paper | Discussion Paper | Discussion Paper |

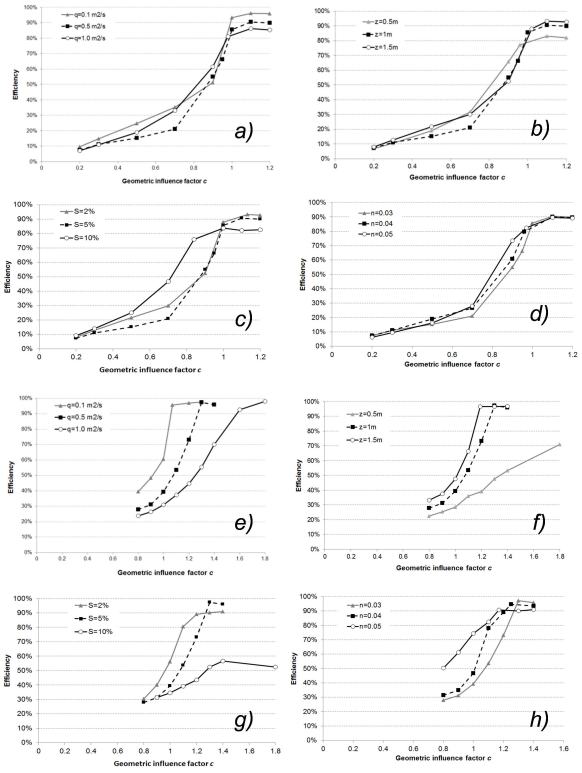

Fig. 6. Efficiency in the reduction of average friction slope as a function of the geometric influence factor c for a range of conditions. n = Manning roughness coefficient; q = unitary discharge; S = bed slope; z = effective check dam height.

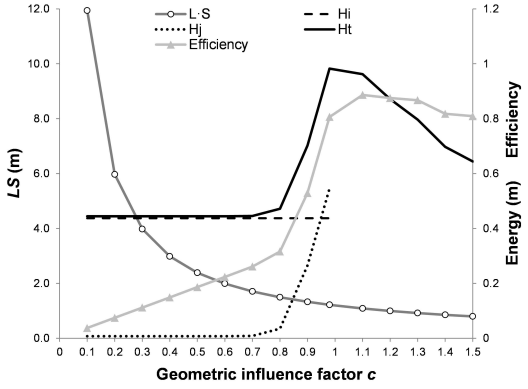

Fig. 7. Profiles of the main energetic parameters as a function of the geometric influence factor c for initial conditions ($q = 0.5\,m^2\,s^{-1}$; $S = 5\,\%$; $n = 0.04$; $z = 1.19$). E_{fs} = efficiency in the reduction of friction slope; H_i = energy dissipated at the impact zone; H_j = energy dissipated at the hydraulic jump; H_t = total energy dissipated ($H_i + H_j$); LS = difference in total head between adjacent dams.

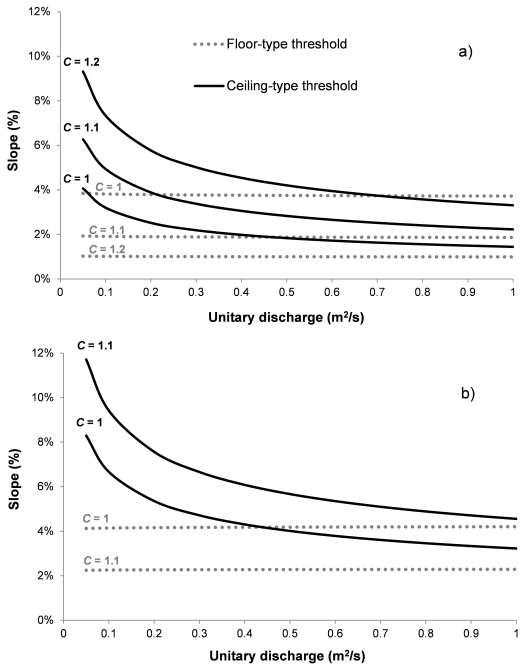

Fig. 8. Threshold curves of optimal *c* for a particular geometric influence factor *c* for initial (grey dotted line) and dam-filling (solid black line) conditions with different roughness coefficients **(a)** $n = 0.04$; **(b)** $n = 0.06$.

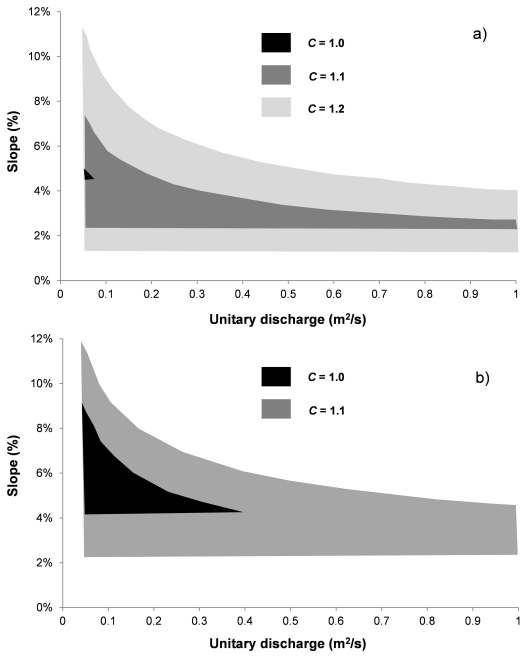

Fig. 9. Regions of optimal efficiency for a particular geometric influence factor *c* valid throughout the lifetime of the structure for different roughness coefficients **(a)** $n = 0.04$; **(b)** $n = 0.06$.

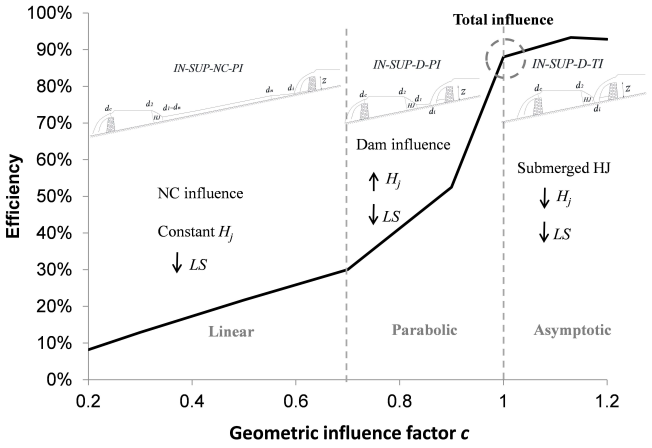

Fig. 10. Conceptual diagram of check dam efficiency as a function of the geometric influence factor *c* for initial conditions.